ORIGINAL ARTICLE

PDZK1 inhibits the development and progression of renal cell carcinoma by suppression of SHP-1 phosphorylation

T Tao[1,5], X Yang[1,2,5], J Zheng[1,2], D Feng[3], Q Qin[1,2], X Shi[1], Q Wang[1], C Zhao[1], Z Peng[1], H Liu[1,2], WG Jiang[4] and J He[1,2]

Renal cell carcinoma (RCC) is one of the most aggressive urologic cancers, however, the mechanism on supporting RCC carcinogenesis is still not clear. By using gene expression profile analysis and functional clustering, PDZ domain-containing 1 (PDZK1) was revealed to be downregulated in human clear cell renal cell carcinoma (ccRCC) samples, which was also verified in several independent public ccRCC data sets. Using PDZK1 overexpression and knockdown models in ccRCC cell lines, we demonstrated that PDZK1 inhibited cell proliferation, cell cycle G1/S phase transition, cell migration and invasion, indicating a tumor-suppressor role in the development and progression of ccRCC. Our study further demonstrated that PDZK1 inhibited cell proliferation and migration of ccRCC via targeting SHP-1. PDZK1 was further identified to suppress cell proliferation by blocking SHP-1 phosphorylation at Tyr536 via inhibition of the association between SHP-1 and PLCβ3, and then retarding Akt phosphorylation and promoting STAT5 phosphorylation in ccRCC cells. Moreover, the inhibitive effects of PDZK1 on SHP-1 phosphorylation and the tumor growth were verified *in vivo* by xenograft tumor studies. Accordingly, PDZK1 expression was negatively correlated with SHP-1 activation and phosphorylation, advanced pathologic stage, tumor weight and size, and prognosis of ccRCC patients. These findings have provided first lines of evidences that PDZK1 expression is negatively correlated with SHP-1 activation and poor clinical outcomes in ccRCC. PDZK1 was identified as a novel tumor suppressor in ccRCC by negating SHP-1 activity.

INTRODUCTION

Renal cell carcinoma (RCC) is an aggressive urologic cancer type. Its incidence increases annually ~ 2%.[1] Clear cell renal cell carcinoma (ccRCC) accounts for 75% of all kidney tumors.[2] Chemotherapy and radiotherapy are less-effective treatments against ccRCC. Recent advances in molecular biology have revealed that angiogenesis and tumor cell proliferation have important roles for the development and progression of ccRCC.[3,4] These findings provide a theoretical basis for ccRCC-targeted therapies and have greatly changed the therapeutic landscape in ccRCC.

It has been well known that inactivation of tumor-suppressor VHL (Von Hippel-Lindau) results in an accumulation of hypoxia-inducible factor (HIF), which contributes to neoangiogenesis in >80% ccRCC.[5,6] Thus, at present, most RCC-targeted drugs are mainly designed to inhibit angiogenic pathways,[7] but have only achieved a limited survival-time improvement.[8] Traditionally, the evaluation of the parameters of tumor cell proliferation including tumor size, mitotic index, proliferation cell nuclear antigen and Ki67 antigen have been suggested as having prognostic importance in RCC.[9] However, the molecular mechanisms on the deregulation of cell proliferation in RCC is still largely unknown. Uncovering these mechanisms may aid in the clarity of the pathogenesis of RCC and advancement of more effective therapy.

Recently, there has been an increasing interesting for the PDZ domain-containing proteins, which have essential roles in tumor growth, development and metastasis.[10] Studies have established that several PDZ proteins including TIP-1, DLG, Erbin and NHERF1 are involved in tumorigenesis such as colorectal and breast cancers.[11–14] The NHERF family of PDZ proteins are commonly expressed in polarized epithelia.[15] Abnormal expression of NHERF1 has been found in several types of tumors, such as hepatocellular carcinoma, breast cancer and nerve schwannoma.[14] NHERF1 expression is also related to cancer invasion and metastasis.[16] Over 150 PDZ proteins have been found in the human proteome, and many of which are highly expressed in renal epithelial cells.[17] However, the roles of PDZ proteins in renal cancer carcinogenesis and progression are largely unknown.

In this study, differential gene expression analysis using the available mRNA expression profile of ccRCC from GEO data set combined with GO analysis was used for the screening of target PDZ proteins associated with cell proliferation. Among 2267 downregulated genes, PDZK1, a member of PDZ proteins, is downregulated and associated with cell proliferation in ccRCC. Loss of PDZK1 is demonstrated to be correlated with advanced clinical stage and adverse prognosis in ccRCC. PDZK1 retarded cell growth and promoted cell cycle arrest of ccRCC cells *in vivo* and *in vitro* by blocking SHP-1 phosphorylation through suppression of SHP-1 binding to PLCβ3. These data support a novel tumor-

[1]Department of Biochemistry and Molecular Biology, Capital Medical University, Beijing, PR China; [2]Beijing Key Laboratory for Cancer Invasion and Metastasis Research, Beijing International Cooperation Base for Science and Technology on China-UK Cancer Research, Capital Medical University, Beijing, PR China; [3]Department of Interventional Radiology, First Hospital of Shanxi Medical University, Taiyuan, PR China and [4]Cardiff China Medical Research Collaborative, Cardiff University School of Medicine, Heath Park, Cardiff, UK. Correspondence: Dr H Liu or Professor J He, Department of Biochemistry and Molecular Biology, Capital Medical University, No.10 Xitoutiao, You An Men, Beijing 100069, PR China.
E-mail: hualh08@ccmu.edu.cn or jq_he@ccmu.edu.cn
[5]These authors contributed equally to this work.

6120

suppressor role of PDZK1 and provide a new insight into the development and progression of ccRCC.

RESULTS

Low expression of PDZK1 predicts poor survival in ccRCC

To identify aberrantly expressed genes associated with ccRCC carcinogenesis and progression, the mRNA expression profile obtained from GSE53757 (http://www.ncbi.nlm.nih.gov/geo/) with 72 paired ccRCC and adjacent non-tumor renal tissues were analyzed. Totally, 2267 genes were significantly downregulated in ccRCC tissues by GEO2R analysis. DAVID (Database for Annotation, Visualization and Integrated Discovery, developed by NIAID/NIH) was then used to investigate gene ontology (GO) term enrichment. GO analysis revealed that 40 genes, related to the biological process of 'cell proliferation', and 10 genes associated with the molecular function of 'PDZ domain binding', were downregulated in ccRCC tissues. Only TGFBR3 and PDZK1 genes were associated to both 'cell proliferation' and 'PDZ domain binding' ($P < 0.001$; Supplementary Figure S1). TGFBR3 has been involved in ccRCC carcinogenesis.[18] However, the role and relevance of PDZK1 in ccRCC are still largely unknown, so we focused on exploring physiological and pathological significance of PDZK1 in this study.

To verify these findings, the expression of PDZK1 mRNA in ccRCC and their adjacent tissues were analyzed either with GEO ccRCC data set or TCGA's RNA-seq data of ccRCC patients; all the results showed that PDZK1 mRNA expression level was obviously downregulated in ccRCC tissues as compared with adjacent non-tumor renal tissues (Figures 1a and b). Further analysis of PDZK1 mRNA levels from five independent published studies in ONCOMINE database entirely confirmed our results that PDZK1 mRNA expression was significantly lower in ccRCC tissues than that in normal renal tissues (Figure 1c). Moreover, analysis of PDZK1 protein expression in tissue microarray of 90 ccRCC specimens also confirmed that PDZK1 expression was reduced in ccRCC tissues at protein level (Figures 1d and e).

To explore the clinical relevance of PDZK1 in ccRCC, the correlation between PDZK1 expression levels and tumor stages was evaluated. The results showed that PDZK1 was negatively correlated with the tumor stage either at protein (Figures 1f, $P < 0.05$) or mRNA (Figures 1g, $P < 0.01$) levels, also tumor weight and volume (Supplementary Figures S2a and b). In addition, we found that PDZK1 was negatively correlated with the T stage, which reflected the tumor size, either at protein (Supplementary Figure S2c, $P < 0.05$) or mRNA (Supplementary Figure S2d, $P < 0.05$) levels. All these data indicate that loss of PDZK1 expression is associated with advanced tumor stage and tumor growth. Also we found that lower PDZK1 expression correlated with poor clinical outcome of ccRCC patients.[19]

PDZK1 inhibits cell proliferation, migration and invasion of ccRCC cells

Tumor cell proliferation is a major representative indicator of malignant phenotypes. PDZK1 was related to cell proliferation by GO analysis using the DAVID online analysis tool, so the effects of PDZK1 expression on ccRCC cell proliferation were investigated.

The 769-P and 786-O ccRCC cells were stably transfected with PDZK1 expression constructs, and the overexpression of PDZK1 was confirmed by western blotting (Figure 2a). Then cell viability and colony formation were measured. The results showed that PDZK1 overexpression in 769-P and 786-O cells led to reduced cell proliferation (Figure 2b) and decreased colonogenicity (Figure 2c). To further confirm the results, PDZK1 was knocked down in 769-P and 786-O cells, by stable transfection with small hairpin RNAs, shPDZK1#1 and shPDZK1#2, respectively. Significantly decreased PDZK1 expression was verificated by western blotting (Figure 2d), and the cell proliferation increased robustly in PDZK1 knockdown

cell lines (Figure 2e). These data confirmed that PDZK1 expression inhibited ccRCC cell proliferation. To explore the possible mechanism of cell proliferation inhibition by PDZK1, we further investigated the effects of PDZK1 on cell cycle progression using flow cytometry. As shown in Figure 2f, after depletion of PDZK1, the percentage of 769-P cells in G0/G1 phase obviously decreased from 66.5 to 48.1%, whereas the distribution of cells in S phase increased from 20.7 to 37.2%. The data demonstrated that PDZK1 induced cell cycle arrest at G1/S checkpoint in ccRCC cells. Taken together, PDZK1 expression inhibited cell growth and promoted cell cycle arrest of ccRCC cells.

The effects of PDZK1 expression on the migration or invasion ability of ccRCC cells were also evaluated by scratch or transwell assays. The results showed that overexpression of PDZK1 in 769-P and 786-O cells inhibited tumor cell migration (Figure 3a) and invasion (Figure 3b) as compared with control cells.

To further verify the pathways associated with the pathogenesis of ccRCC, the patients were stratified by the median levels of PDZK1 and gene set enrichment analysis (GSEA) was performed with TCGA ccRCC data sets; data showed that the gene signatures of cell proliferation, cell cycle and migration were enriched in patients with low PDZK1 expression, suggesting that PDZK1 repressed cell proliferation and migration abilities in ccRCC tissues (Supplementary Figure S3). Taken together, our results indicate that PDZK1 elicits a tumor-suppressive role via regulation of cell proliferation and migration in ccRCC.

PDZK1 inhibits cell proliferation and migration of ccRCC via targeting SHP-1

The PTPase (phosphatase) activity of SHP-1 has an important role in cell proliferation and migration,[20] so the roles of SHP-1 in PDZK1-mediated proliferation and migration were studied in ccRCC cells. NSC-87877, a potent inhibitor of SHP-1 phosphatase, was used to inhibit the SHP-1 activity in 769-P cell. As shown in Figure 4, the proliferation of 769-P cells was dose- and time-dependently inhibited by NSC-87877, suggesting that SHP-1 activity is essential for ccRCC cell proliferation (Figures 4a and b). To illuminate whether PDZK1 suppresses ccRCC cell proliferation and migration by targeting SHP-1, cell proliferation and migration assays were performed by treating the 769-P cells with NSC-87877 in the presence or absence of PDZK1. PDZK1 showed no effects on the proliferation and migration of 769-P cells when SHP-1 activity was inhibited by NSC-87877 (Figures 4c and d). To confirm these results, cell proliferation in 769-P cells was detected after combined knockdown of PDZK1 and SHP-1. The results showed that silencing PDZK1 expression significantly promoted cell proliferation in 769-P cells when SHP-1 existed. However, PDZK1 had no effects on cell proliferation when SHP-1 was knocked down (Figure 4e). Taken together, these data indicated that PDZK1 inhibits cell proliferation and migration of ccRCC by targeting SHP-1.

PDZK1 inhibits SHP-1 phosphorylation at Tyr536 via suppression of SHP-1/PLCβ3 binding, leading to reduction of Akt phosphorylation and promotion of STAT5 phosphorylation in ccRCC cells

Lines of evidences showed that phosphatase activity of SHP-1 was regulated by SHP-1 phosphorylation.[21] To explore the regulatory mechanism of PDZK1 on SHP-1 activity, PDZK1 expression was changed by overexpression or knockdown in 786-O cells and SHP-1 phosphorylation was detected. As shown in Figures 5a and b, PDZK1 overexpression suppressed Tyr536 phosphorylation of SHP-1 in a dose-dependent manner. Conversely, PDZK1 knockdown increased the SHP-1 phosphorylation in 786-O cells (Figure 5c). Consistently, the inhibitive effects of PDZK1 on SHP-1 phosphorylation were verified in 769-P cells (Supplementary Figure S4).
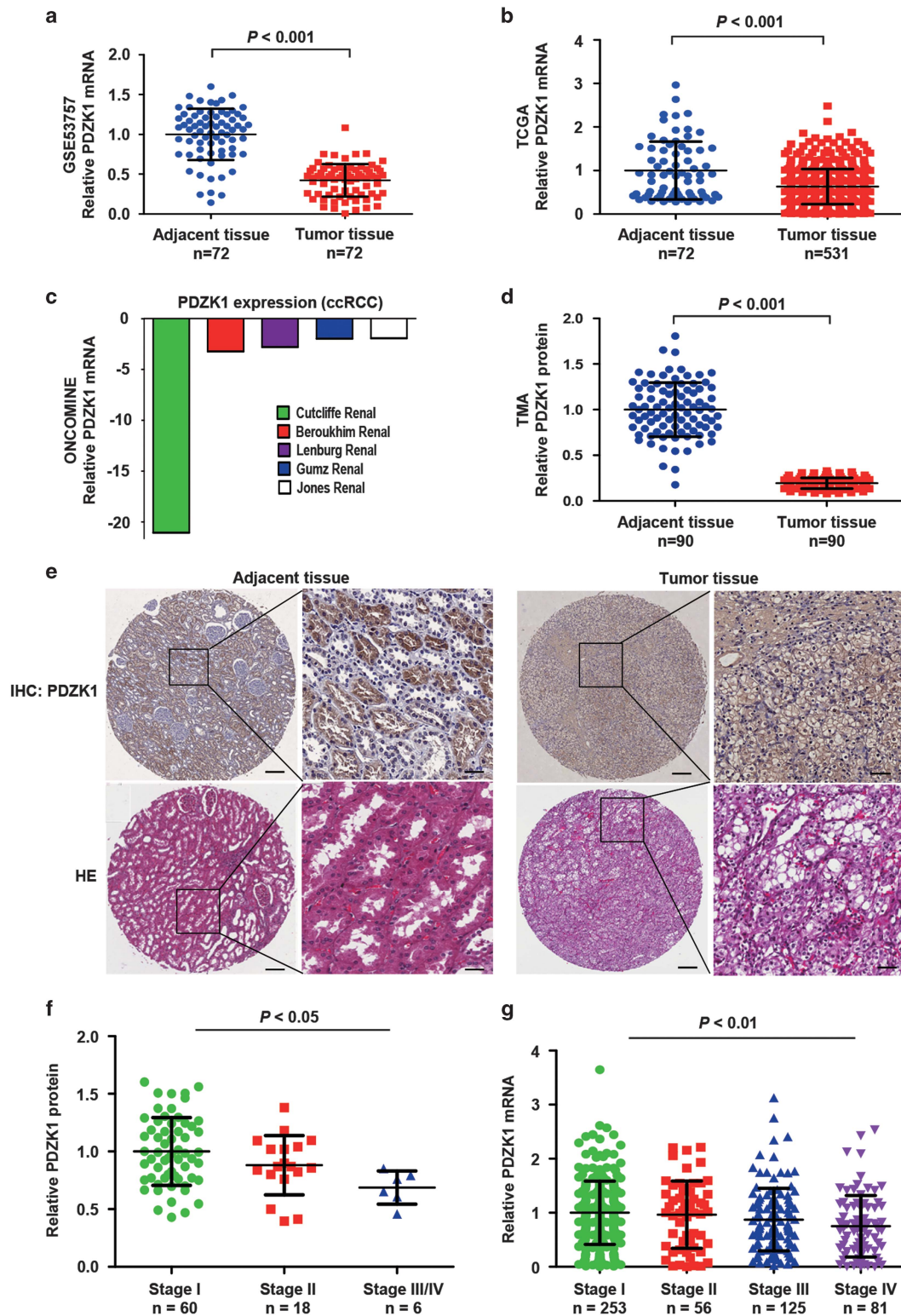
Figure 1. PDZK1 expression is downregulated and negatively associated with advanced tumor stages of patients with ccRCC. (**a**, **b**) Scatter plots of fold change of PDZK1 mRNA expression in ccRCC and their adjacent tissues, the data were obtained from GSE53757 (**a**), or from TCGA ccRCC data set (**b**) (nonparametric Mann–Whitney test, $P < 0.001$). (**c**) Fold change of PDZK1 mRNA expression in ccRCC compared with normal renal tissues, the data were obtained from five independent studies published in ONCOMINE database. (**d**) PDZK1 protein levels in 90 human ccRCC and normal renal tissue samples were analyzed by immunohistochemistry with tissue microarray (TMA) (nonparametric Mann–Whitney test, $P < 0.01$). (**e**) Representative images of PDZK1 immunohistochemical staining in ccRCC (Right) and its adjacent tissue (Left). Scale bars, 200 μm and 50 μm. H&E, hematoxylin and eosin. (**f**, **g**) Advanced tumor stages is associated with lower PDZK1 protein levels by a TMA study of ccRCC patient specimens (**f**), or lower PDZK1 mRNA levels, with data obtained from TCGA ccRCC data sets (**g**). Data were analyzed by one-way ANOVA, $P < 0.05$.
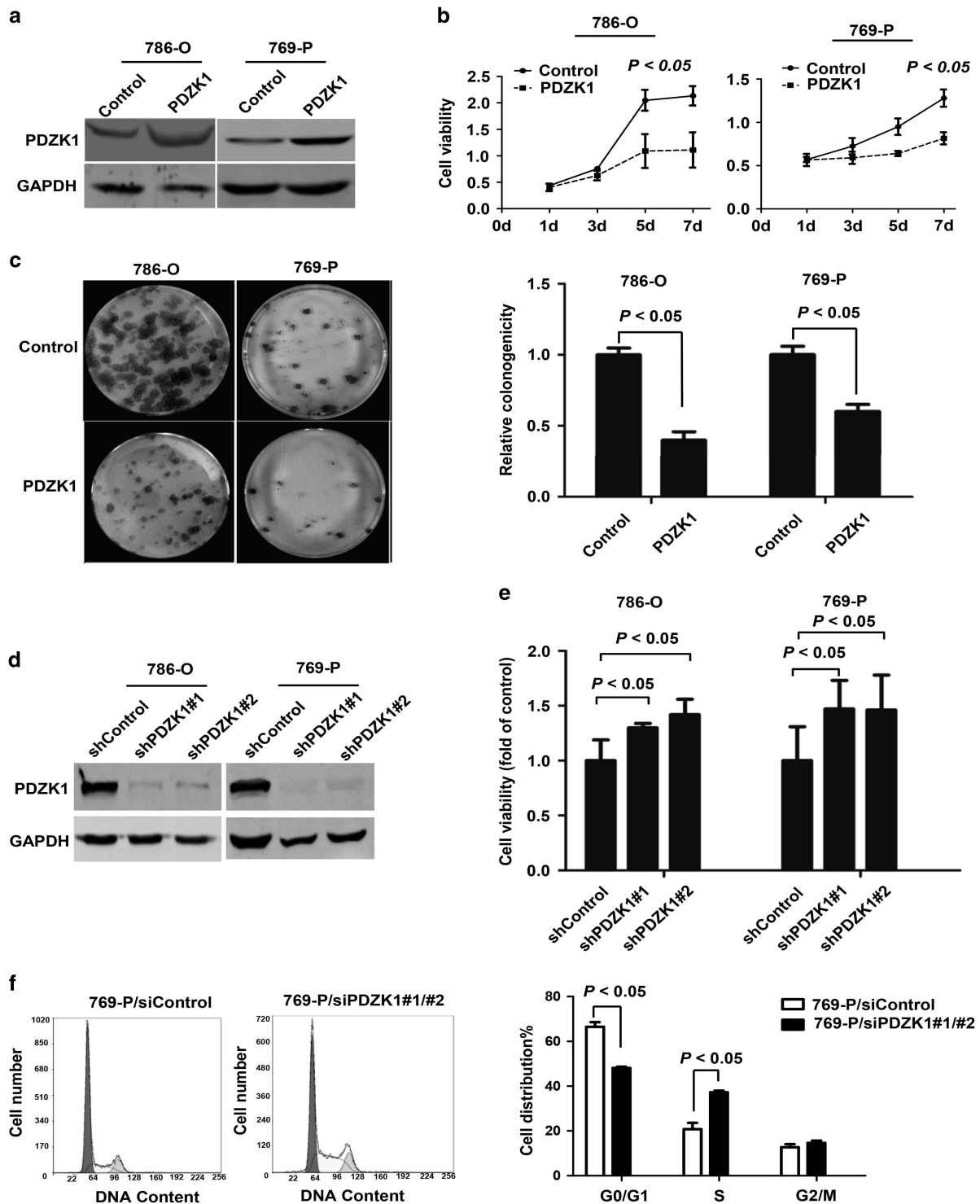
Figure 2. PDZK1 inhibits the proliferation of ccRCC cells. (a) Overexpression of PDZK1 in 786-O and 769-P cells was verified by immunoblotting analysis; GAPDH was used as a loading control. (b) PDZK1 overexpression significantly reduced cell proliferation of 786-O and 769-P cells by CCK8 viability assays (Repeated-measures analysis of variance, $P < 0.05$). (c) PDZK1 inhibited the colony formation of 786-O and 769-P cells. Left panel: Representative photographs of the colonogenicity. Right panel: Quantification of the colony formation efficiency. $P < 0.05$ vs control. (d) PDZK1 knockdown by stable transfection of shRNA in 786-O and 769-P cells, respectively, was confirmed by western blotting. (e) PDZK1 knockdown enhances cell proliferation in 786-O and 769-P cells. PDZK1 shRNA-transfected 786-O or 769-P cells were, respectively, cultured in 96-well plates and stained with CCK8 at 72 h. Growth of 786-O and 769-P cells was assessed by measuring absorbance at 450 nm with a spectrophotometer. Values were expressed as fold change compared with scrambled control shRNA-transfected cells ($P < 0.05$). (f) PDZK1 knockdown led to S phase accumulation in 769-P cells. Cell transfected with mixed two PDZK1 siRNAs and cell cycle analysis was performed using propidium iodide DNA staining and flow cytometry (t-test, $P < 0.01$). All data were representatives of at least three independent experiments.
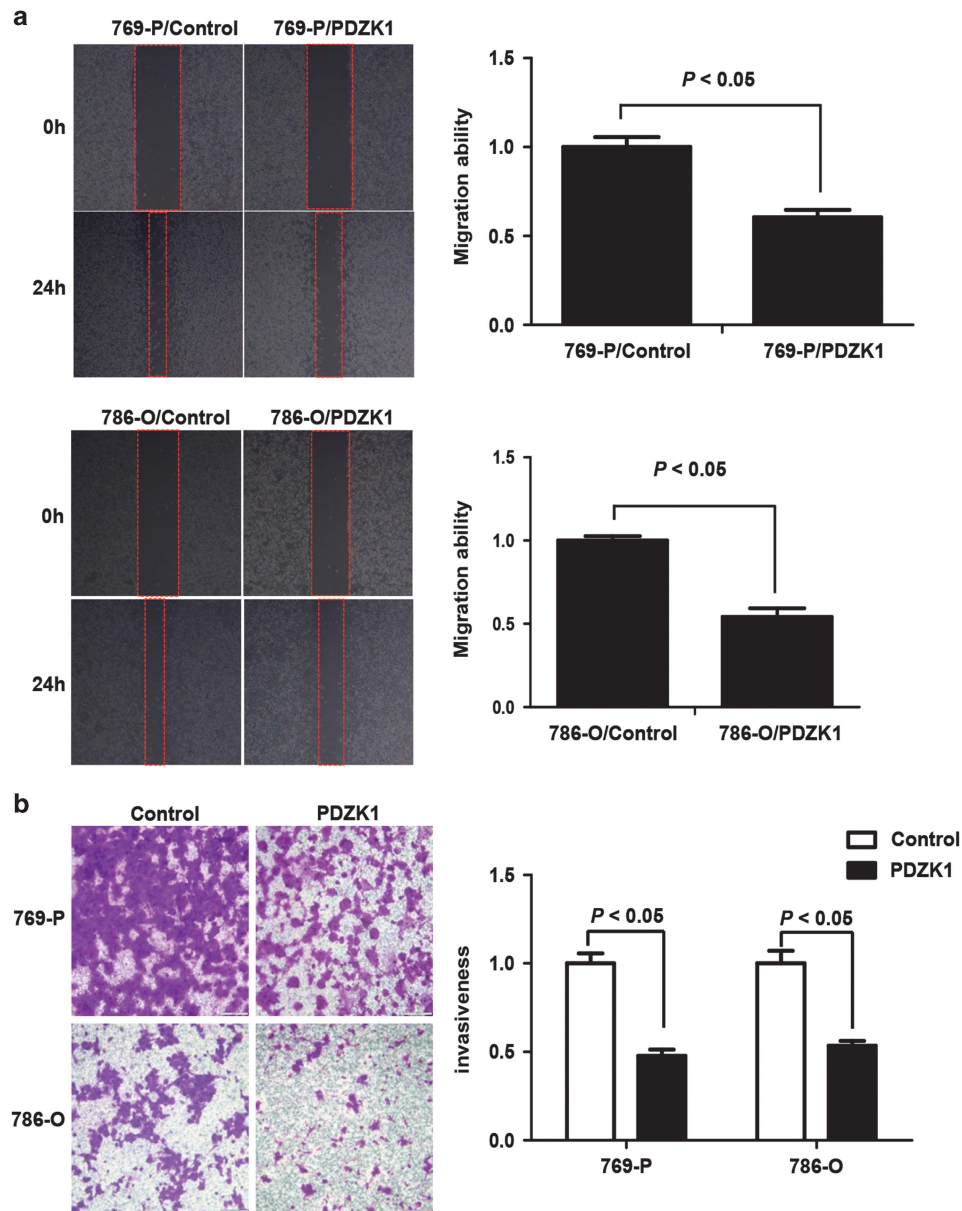
Figure 3. PDZK1 inhibits ccRCC cell migration and invasion. (**a**) PDZK1 overexpression inhibited cell migration by wound-healing assay. The relative migration distance was quantified (right panel) (*t*-test, $P < 0.01$). (**b**) PDZK1 overexpression inhibited cell invasion. The Boyden chambers invasion assay was used. Invasive cells are represented as mean ± s.d. (*t*-test $P < 0.01$). All data were representatives of at least three independent experiments.

The previous report showed that SHP-1 phosphorylation was regulated by PLCβ3.[22] Therefore, we further explored the potential roles of PLCβ3 in PDZK1-mediated suppression on SHP-1 phosphorylation. As the results shown in Figure 5d, knockdown of PLCβ3 robustly abolished SHP-1 phosphorylation at Tyr536 in 786-O cells, and PDZK1 knockdown significantly increased SHP-1 phosphorylation only when PLCβ3 existed. These results suggested that PDZK1 inhibition of SHP-1 phosphorylation at Tyr536 required PLCβ3.

SHP-1 phosphatase activity was generally assessed by the impact on phosphorylation of its target molecules such as STAT3, STAT5 and Akt.[20,22,23] To identify the cellular targets of SHP-1 in renal cancer cells, the phosphorylation of STAT3 , STAT5 and Akt were explored in 769-P cells, in which PDZK1 was overexpressed and knocked down, respectively. The results showed that PDZK1 significantly promoted STAT5 phosphorylation, and robustly

inhibited Akt phosphorylation, with no detectable impact on STAT3 phosphorylation (Figures 6a and b). To further confirm our initial findings, the correlation between PDZK1 mRNA levels and activation of Akt or STAT3 signaling in ccRCC specimens was investigated by GSEA. The results demonstrated a negative correlation between PDZK1 level and the activation of Akt signaling (Figure 6c), but no correlation between PDZK1 and STAT3 activation was found in ccRCC samples (Figure 6d). The data are in line with the results of our *in vitro* study. Unfortunately, a gene set of STAT5 signaling activation was currently not available yet, we were therefore unable to detect the correlation of PDZK1 with STAT5 signaling activation in ccRCC specimens. Taken together, our results indicate that PDZK1/SHP-1 inhibits ccRCC development and progression by regulation of Akt signaling, including possibly STAT5 signaling. These need to be validated with further studies.
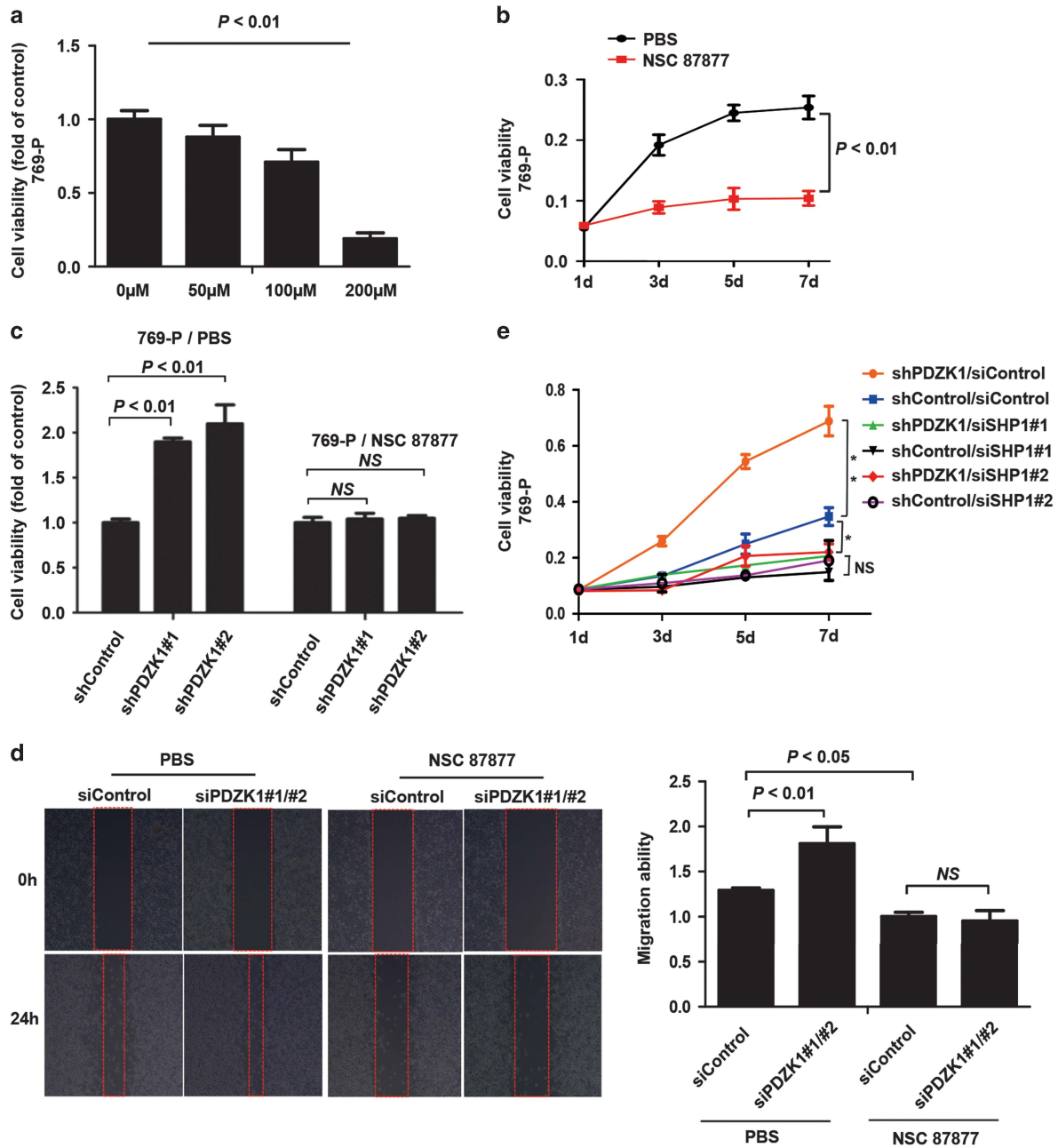
Figure 4. PDZK1 inhibits cell proliferation and migration of ccRCC via targeting SHP-1. (**a**) NSC-87877, a SHP-1 selective inhibitor, retarded 769-P cell proliferation in a dose-dependent manner. 769-P cells were cultured in 96-well plates and treated with different concentrations of NSC-87877 ($0 \sim 200$ μM) for 72 h, respectively. Viability of the cells was assessed by CCK8 assay by measuring absorbance at 450 nm with a spectrophotometer. Data were analyzed by one-way ANOVA ($P < 0.01$). (**b**) Time course of the 769-P cells growth with NSC-87877 (100 μM) treatment as indicated. 769-P cells were incubated with NSC-87877 at indicated time points, and cell proliferation was measured by CCK8 viability assays as described previously (Repeated-measures analysis of variance, $P < 0.05$). (**c**) PDZK1 inhibited 769-P cell growth through suppressing SHP-1 activation. 769-P and 769-P-shPDZK1 cells were cultured in 96-well plates, respectively, and treated in the presence or absence of SHP-1 inhibitor NSC-87877 (100 μM) for 72 h, then stained with CCK8. Viability of 769-P cells was assessed by measuring absorbance at 450 nm with a spectrophotometer. Values were represented relative to the absorbance compared with scrambled control. (**d**) PDZK1 inhibited 769-P cell migration through suppressing SHP-1 activation. 769-P cells transfected with siRNA control or two mixed PDZK1 siRNAs were cultured, respectively, and treated in the presence or absence of SHP-1 PTPase inhibitor NSC-87877 (100 μM) for 24 h. The migration of wound-healing assay was subsequently calculated (t-test, $P < 0.05$). (**e**) PDZK1 inhibited 769-P cell growth dependent on SHP-1 expression. 769-P and 769-P-shPDZK1 cells were transfected with either SHP-1 siRNA#1, siRNA#2 or scramble control, respectively, and cell proliferation was determined as described in Figure 2b. All data were representatives of three independent experiments and data are shown as mean ± s.d. *$P < 0.05$, **$P < 0.01$.

Studies have shown that PLCβ3 bond SHP-1 via C-terminal of PLCβ3 to facilitate the SHP-1 phosphorylation at Tyr536.[22] Meanwhile, PLCβ3 can also interact with PDZK1 via its PDZ-binding motif at the C-terminus.[24] Our results also verified these interactions endogenously in 786-O cell (Figures 7a and b), and deletion of the PDZ-binding motif in C-terminus of PLCβ3 (PLCβ3-△NTQL) completely abolished its interaction with PDZK1 (Figure 7c). Interestingly, the mutation of PLCβ3-ΔNTQL
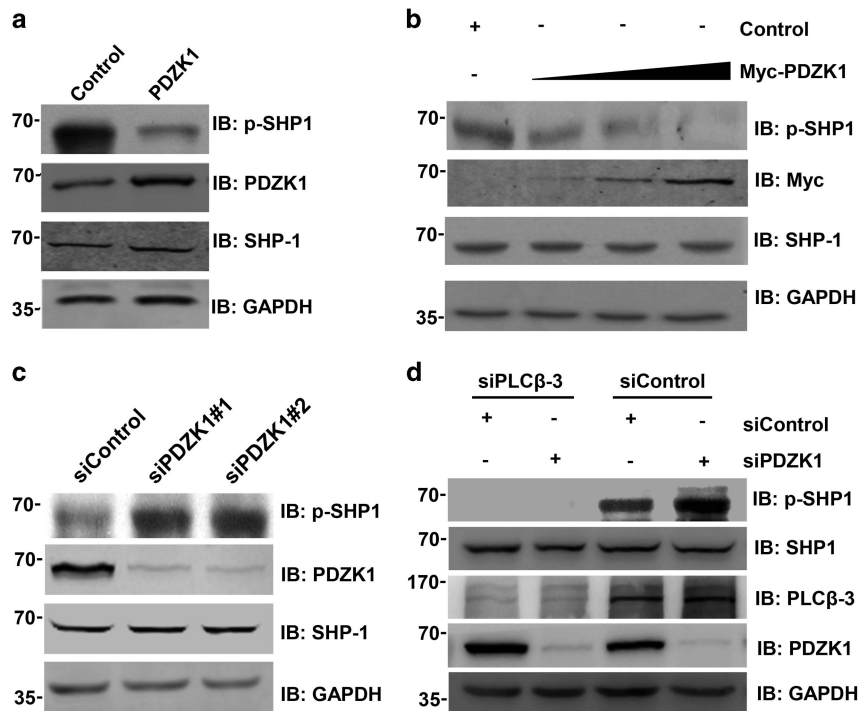
Figure 5. PDZK1 blocks SHP-1 phosphorylation at Tyr536. (**a**) PDZK1 overexpression reduced SHP-1 phosphorylation. After 24 h of transfection with constructs of myc-PDZK1 or control vectors in 786-O cells, the endogenous SHP-1 phosphorylation at Tyr536 was detected by immunoblotting. (**b**) PDZK1 decreased the SHP-1 phosphorylation at Tyr536 in a dose-dependent manner. After 24 h transfection with increased amounts of constructs of myc-PDZK1 or control vectors in 786-O cells, the SHP-1 phosphorylation at Tyr536 and total SHP-1 were detected by immunoblotting. (**c**) Knockdown of PDZK1 expression increased SHP-1 phosphorylation in 786-O cells. 786-O cells transfected with either PDZK1 siRNA or scramble control, and the SHP-1 phosphorylation at Tyr536 was determined. Total expression levels of SHP-1 and GAPDH were shown as loading controls. (**d**) Inhibition of SHP-1 phosphorylation by PDZK1 required PLCβ3 expression. 786-O sicontrol and 786-O siPDZK1 cells were transfected with either PLCβ3 siRNA or scramble control respectively, and the SHP-1 phosphorylation at Tyr536 in 786-O cells was determined. Total expression levels of SHP-1 and GAPDH were shown as loading controls. All data were representative of three independent experiments.

significantly enhanced the association of PLCβ3 and SHP-1 (Figure 7d); reminding that interaction between PDZK1 and PLCβ3 retarded the association of SHP-1 and PLCβ3. To verify this result, GST-PLCβ3-CT was used to pull down endogenous SHP-1 in the absence or presence of different doses of His-PDZK1-PDZ1. As shown in Figure 7e, the PDZ1 domain of PDZK1 exhibited a dose-dependent inhibition of the association between PLCβ3 and SHP-1. This result was further confirmed in HEK293T cells by co-transfection of Flag-PLCβ3 with different amounts of Myc-PDZK1 constructs. Immunoprecipitation of Flag-PLCβ3 followed by western blotting analysis of SHP-1 revealed that SHP-1 co-immunoprecipitation with PLCβ3 was concordantly reduced with a gradual increase of PDZK1 protein level (Figure 7f). Taken together, these results indicate that PDZK1 retards SHP-1 phosphorylation via inhibiting the association between SHP-1 and PLCβ3.

PDZK1 inhibits the ccRCC cell proliferation *in vivo* by blocking SHP-1 phosphorylation

To examine the roles of PDZK1 *in vivo*, a model of xenograft tumor was generated through subcutaneously injecting PDZK1 over-expressed or control ccRCC cells into nude mice. Overexpression of PDZK1 suppressed the growth of ccRCC xenografts within 16 days (Figure 8a). Accordingly, the weight and volume of tumors were significantly decreased in PDZK1 overexpressed group as compared with the control (Figures 8b–d). Immunohistochemical staining analysis showed that PDZK1 overexpression decreased the Tyr536 phosphorylation of SHP-1, and reduced the expression

of Ki67, the cell proliferation marker (Figure 8e). These results suggest that PDZK1 suppresses tumor cell proliferation by inhibiting the phosphorylation of SHP-1 in xenograft tumor of ccRCC cells.

To further explore the correlation of PDZK1 and SHP-1 phosphorylation in ccRCC tissues, the expression levels of PDZK1 and phosphorylated SHP-1 were examined with western blotting. As compared with the paracancerous tissues, PDZK1 protein level was markedly decreased in ccRCC tissues. Accordingly, SHP-1 phosphorylation levels were significantly increased in ccRCC tissues (Figure 9a).

To delineate relevance of SHP-1 activation in ccRCC development and progression, gene signatures in response to SHP-1 activation were analyzed in TCGA database of ccRCC patients. Data showed that the gene signatures specific to SHP-1 activation were enriched in ccRCC patients with cancer or poor prognosis (Figure 9b and c), suggesting that SHP-1 activation was positively associated with ccRCC development and progression. To further verify whether loss of PDZK1 expression is associated with SHP-1 activation, GSEA was also used to test the enrichment value of SHP-1 activation related with PDZK1 mRNA levels. Results showed that gene signatures of SHP-1 activation were positively enriched in PDZK1 low expression group (false discovery rate = 0.001) (Figure 9d). These findings provide first lines of evidences that PDZK1 levels are negatively correlated with SHP-1 activation, suggesting that loss of PDZK1 in ccRCC patients may contribute to the tumorigenesis and progression of ccRCC via activation of SHP-1 (Figure 9e).
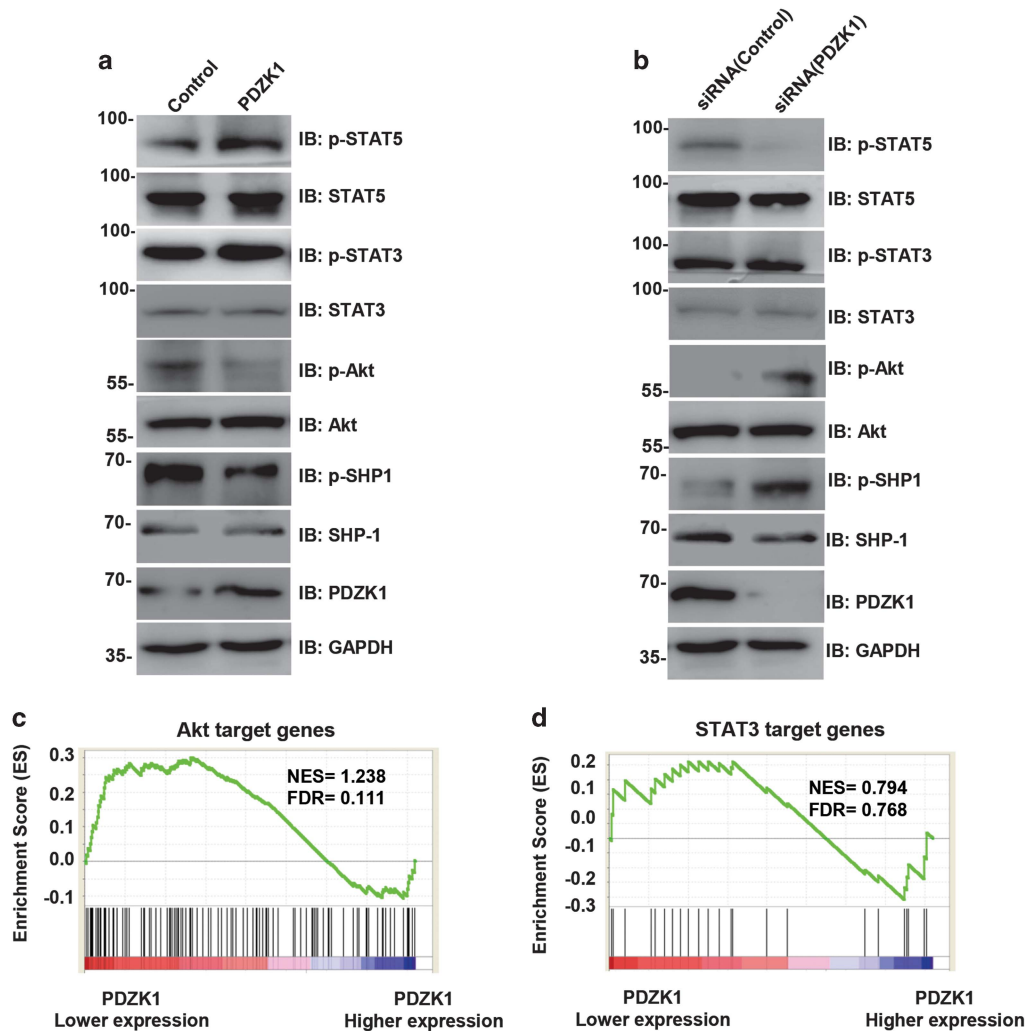
Figure 6. PDZK1/SHP-1 regulates Akt and STAT5 signaling in ccRCC cells. (**a**) PDZK1 overexpression retarded Akt phosphorylation, and promoted STAT5 phosphorylation. After 24 h transfection with constructs of myc-PDZK1 or control vectors in 769-P cells, the phosphorylation of Akt, STAT5, STAT3 and SHP-1 was detected by immunoblotting. (**b**) Knockdown of PDZK1 expression increased Akt phosphorylation and decreased STAT5 phosphorylation in 769-P cells. 769-P cells were transfected with either two mixed PDZK1 siRNAs or scramble control for 48 h, the phosphorylation of Akt, STAT5, STAT3 and SHP-1 was detected by immunoblotting. Total protein contents of Akt, STAT5, STAT3 and SHP-1 were shown as loading controls. (**c**, **d**) Enrichment plots of gene expression signatures for Akt (**c**), and STAT3 (**d**) pathway activation according to PDZK1 mRNA expression levels by GSEA of TCGA ccRCC database. The ccRCC samples were divided into high and low PDZK1 expression groups based on the median values of PDZK1 RNA-seq quantification results. The results showed that PDZK1 level had significant negative correlation with Akt activation (FDR = 0.111), but no correlation with STAT3 activation (FDR = 0.768) in ccRCC samples.

DISCUSSION

Aberrant PDZK1 expression has been observed in several kinds of cancers, and it is involved in tumor cell signaling via its PDZ domain mediated protein-protein interaction.[25,26] However, the role and relevance of PDZK1 in renal cancer are largely unknown. Here, we identified PDZK1 as a downregulated gene in ccRCC through the analysis of mRNA expression profile obtained from the GEO series GSE53757, and revealed PDZK1 as a cell proliferation-related PDZ protein by functional clustering analysis. We provided the evidences that PDZK1 has tumor-suppressive roles in ccRCC. PDZK1 was significantly decreased in ccRCC at mRNA and protein levels. Loss of PDZK1 was in positive correlation with advanced tumor stage and larger tumor size of ccRCC (Figure 1 and Supplementary Figure S2). Studies in ccRCC cells revealed that PDZK1 overexpression inhibited cell proliferation, migration and invasion (Figure 2 and Figure 3), whereas PDZK1 knockdown enhanced cell proliferation (Figures 2d and e). Furthermore, PDZK1 overexpression inhibited tumor growth of

xenografts derived from ccRCC cells in nude mice (Figure 8). These findings support that PDZK1 plays a crucial role in renal carcinogenesis and progression.

It is well known that PDZK1 can interact with multiple proteins and regulate downstream cell signaling.[24,27] Here we showed that PDZK1 interacts with PLCβ3 and affects SHP-1 activation. SHP-1, a member of protein tyrosine phosphatases (PTPs), is previously reported to be largely expressed in the hematopoietic cells and has a role as a tumor suppressor.[28] In solid tumors, SHP-1 is also broadly expressed, however, its expression has been found to correlate with worse survival of breast cancer, glioma and prostate cancer.[20,29,30] It indicates that SHP-1 had tumor-promoting activity in solid tumors. In this study, we found that suppression of SHP-1 activation or expression by its selective inhibitor NSC-87877 or siRNA retarded ccRCC cell proliferation and migration. Also we showed that PDZK1 suppressed cell proliferation, migration of ccRCC cells by targeting SHP-1 (Figure 4). To explore the molecular mechanism by which SHP-1 regulates the renal cancer cells, the
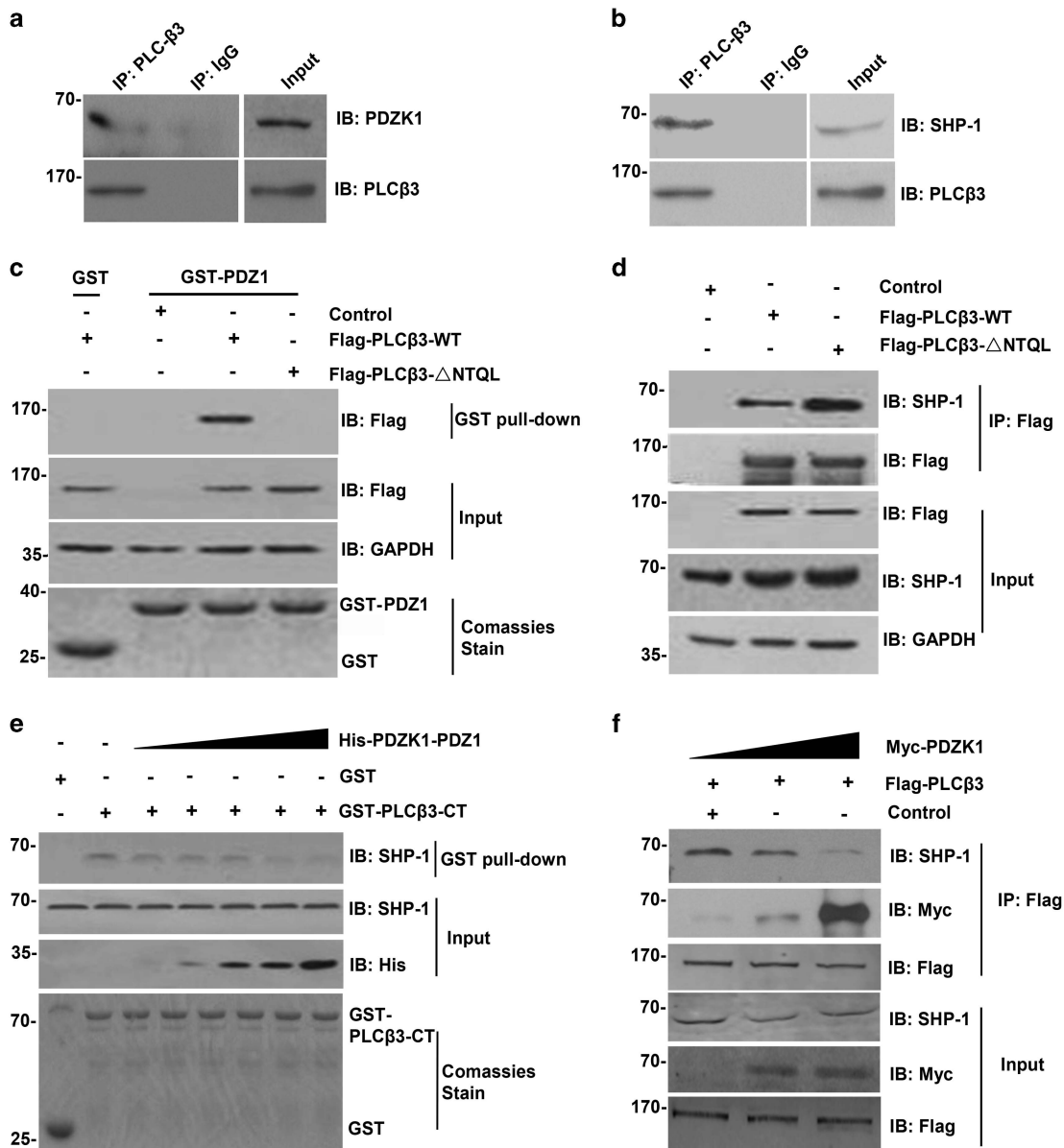
Figure 7. PDZK1 impairs the association between SHP-1 and PLCβ3. (**a**) PDZK1 associated with PLCβ3 in 786-O cells. The cell lysates of 786-O cells were immunopreciptated with rabbit IgG or anti-PLCβ3 monoclonal antibodies, and then the co-immunopreciptation of PDZK1 with PLCβ3 was determined by immunoblotting with anti-PDZK1 antibodies. (**b**) PLCβ3 associated with SHP-1 in 786-O cells. The cell lysates of 786-O cells were immunopreciptated with rabbit IgG or anti-PLCβ3 monoclonal antibodies, and then the SHP-1 co-immunopreciptation with PLCβ3 was determined by immunoblotting with anti-SHP-1 antibodies. (**c**) The carboxyl terminal of PLCβ3 was essential for PLCβ3 binding to PDZK1. COS7 cells were transfected with PLCβ3 wild-type (Flag-PLCβ3-WT) or its deletion mutant lacking PDZ-binding motif (Flag-PLCβ3-ΔNTQL). Cell lysates were pulled down with GST-PDZ1 domain of PDZK1 and GST fusion proteins. The pulled down PLCβ3 was detected by western blotting with anti-Flag antibody (top panel). (**d**) The mutation of PDZ-binding motif deletion in PLCβ3 increased the association of PLCβ3 and SHP-1. 786-O cells were transfected with constructs of Flag-PLCβ3-WT or Flag-PLCβ3-ΔNTQL. Cells were solubilized and incubated with anti-Flag antibody coupled to beads. Co-immunoprecipitation of SHP-1 with Flag-PLCβ3 was detected by western blotting with anti-SHP-1 antibodies. (**e**) The interaction of SHP-1 and PLCβ3 was inhibited by PDZ1 domain of PDZK1 in a dose-dependent manner. Endogenous SHP-1 of ACHN cells was pulled down with GST fusion proteins of wild-type PLCβ3 in the presence of different amount of purified His-PDZK1-PDZ1 protein. SHP-1 in the pulled down complexes was detected by western blotting. (**f**) Full-length PDZK1 inhibited the interaction of SHP-1 and PLCβ3 in a dose-dependent manner in cells. HEK293T cells were transfected with Flag-PLCβ3 plasmid (1 μg) and increased amount of Myc-PDZK1 plasmid (0, 0.5, 1 μg). After 24 h transfection, cells lysates were immunoprecipitated with anti-FLAG antibodies. Co-immunoprecipitations of SHP-1 and PDZK1 were analyzed by western blotting. All data were representatives of three independent experiments.

activation or phosphorylation of potential target proteins of SHP-1, such as Akt, STAT3 and STAT5, and the levels of total tyrosine phosphorylation were detected. Our results showed that no significant change was found in either levels of total tyrosine phosphorylation or STAT3 phosphorylation in ccRCC cells with SHP-1 or PDZK1 knockdown, as well as in the cell pretreated with

NSC-87877 (Supplementary Figure S5). However, with either overexpression or knockdown in 769-P cells, PDZK1 was demonstrated to inhibit Akt phosphorylation, and promote STAT5 phosphorylation. Rodríguez-Ubreva FJ et al.[20] previously reported that SHP-1 promoted Akt Ser473 phosphorylation via inhibiting Tyr phosphorylation of p110 catalytic subunit of PI3K, our results
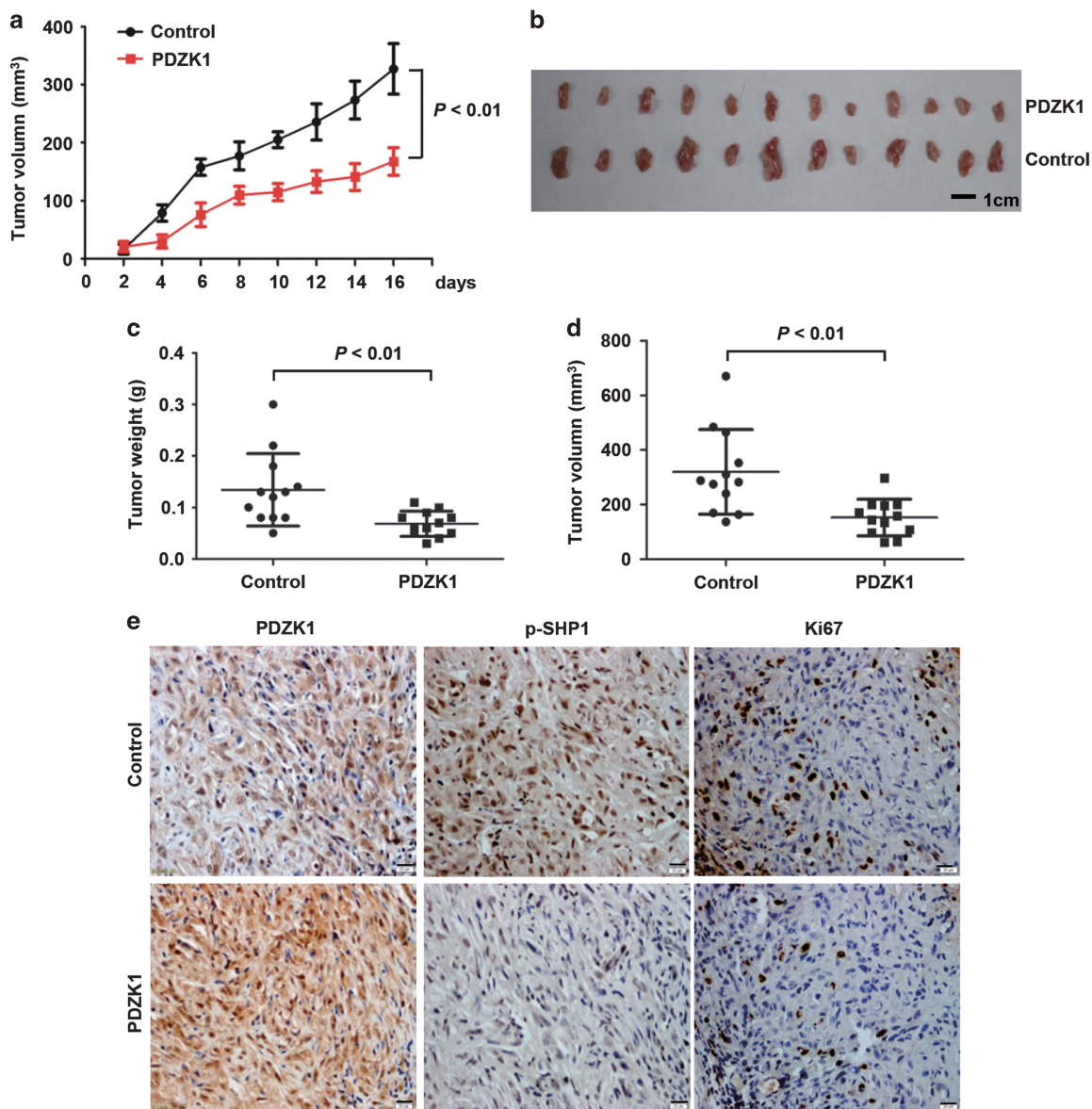
Figure 8. PDZK1 inhibits tumor growth and SHP-1 phosphorylation in xenograft tumors. (**a**) The growth curve of subcutaneous xenograft tumor from ACHN cells in nude mice. ACHN or ACHN-PDZK1 cells were subcutaneously injected into nude mice. Tumor size was measured every 2 days. Values were presented as the mean ± s.d. of 12 mice in each group. (Repeated-measures analysis of variance, $P < 0.01$) (**b**) The dissected tumors from the xenografted mice inoculated with ACHN-PDZK1 or control cells. Mice were sacrificed at a minimum of 16 days after transplantation. (**c, d**) Mean tumor weights and tumor volumes of ACHN-PDZK1 group were significantly smaller than those in the ACHN control group. Xenograft tumors were dissected, and their weight and volumes were measured and comparative analyzed between PDZK1 overexpression group and control group of nude mice. (**e**) IHC staining of PDZK1, pSHP-1 and Ki67 of the PDZK1 overexpressed or control xenografts were shown. Scale bar represented 20 μm, respectively.

suggested that PDZK1 retarded Akt phosphorylation possibly via regulating SHP-1-PI3K-Akt pathway. This negative correlation between PDZK1 and Akt activation was also confirmed in the result analyzed with clinical ccRCC specimens using GSEA method (Figure 6c).Take together, these data indicate that PDZK1 or SHP-1 is unable to alter general tyrosine phosphorylation; however, SHP-1 could selectively dephosphorylate some specific target proteins as Akt or STAT5, and then inhibit ccRCC development and progression. These results need to be validated with further studies.

SHP-1 is composed of two tandem domains of N-SH2 and C-SH2, followed by the catalytic domain of PTP and C-terminal tail, which contains key tyrosine phosphorylation sites in the regulation of SHP-1 activity.[21] N-SH2 is located closely to the PTP catalytic domain of SHP-1, which restricts accession of PTP catalytic domain and

substrate of phosphatase. When SHP-1 Tyr536 phosphorylated, the PTP catalytic domain was separated from N-SH2 to become accessible for its substrates (Figure 9e). This is confirmed by that reduced SHP-1 phosphorylation at Tyr536 results in a drastic reduction of SHP-1 phosphatase activity.[22]

Recent reports reveal that PLCβ3 acts as a scaffold to associate with SHP-1 and recruits tyrosine kinase to phosphorylate SHP-1 by forming a macromolecular complex.[22] In the current study, we showed that PLCβ3 knockdown inhibited SHP-1 phosphorylation in ccRCC cells (Figure 5d), indicating that PLCβ3 is required for the SHP-1 phosphorylation at Tyr536. Our study also showed that PDZK1 dose-dependently inhibited SHP-1 phosphorylation through blocking the association between SHP-1 and PLCβ3 (Figures 5a and b, Figures 7e and f). Taken together, our data
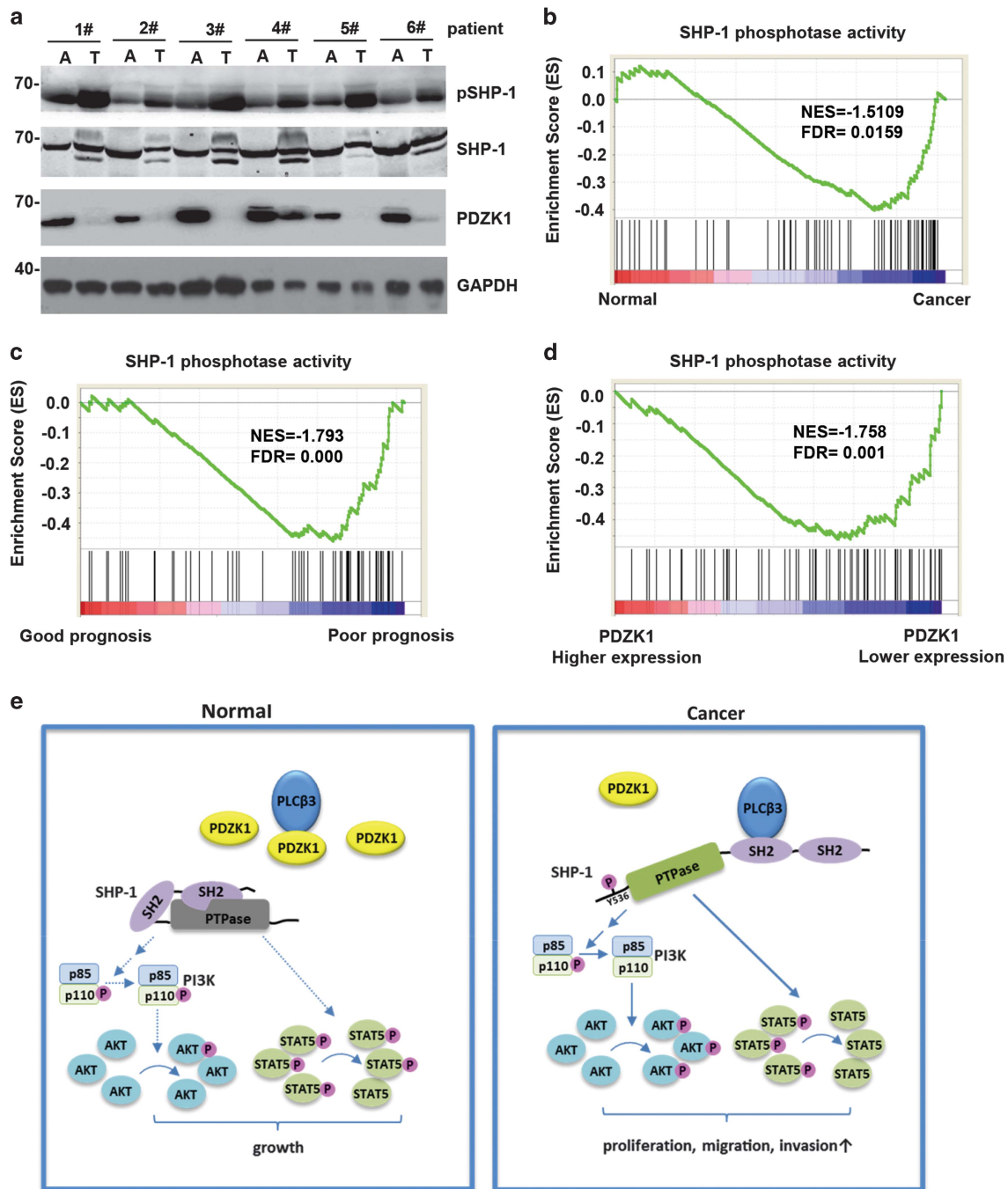
Figure 9. SHP-1 PTPase activity is upregulated in ccRCC, positively correlated with poor prognosis and negatively correlated with PDZK1 expression levels in ccRCC patients. (**a**) Negative correlation between expression levels of PDZK1 and SHP-1 phosphorylation. The expression levels of PDZK1 and phosphorylated SHP-1 of ccRCC specimens and their adjacent tissues were analyzed by western blotting, and total expression levels of SHP-1 and GAPDH were shown as loading controls. (**b**–**d**) SHP-1 is activated in ccRCC, and its activity is positively correlated with poor prognosis and low PDZK1 expression of ccRCC. The gene signatures of SHP-1 activation was significantly enriched in ccRCC, poor prognosis and low PDZK1 expression groups as compared with normal, good prognosis and high PDZK1 expression groups, respectively. (**e**) Schematic illustration of the mechanism of the enhancement of SHP-1 phosphorylation owing to loss of PDZK1 and its association with PLCβ3 in ccRCC.

suggest that PDZK1 inhibits SHP-1 phosphorylation by suppression of the association between SHP-1 and PLCβ3.

As a member of PLCβ family, PLCβ3 generally has its function via the phospholipase activity-dependent pathway.[31] Recently, studies have shown that PLCβ3 can also act as a scaffold to recruit some tyrosine kinases via its non-catalytic C-terminal domain to facilitate SHP-1 phosphorylation.[22] In this study,

we found that PDZK1 retarded SHP-1 phosphorylation via the inhibition of the association between SHP-1 and PLCβ3. Interestingly, PLCβ3 is found to be upregulated and correlated with poor prognosis in renal cancer patients (data not shown). These results are consistent with the finding that upregulated PLCβ3 increased the phosphorylation of SHP-1 in ccRCC cells, indicating that PLCβ3 may have a tumor-promoting role in

6130

renal cancer. However, this hypothesis need to be further explored.

In this study, we found that PDZK1 was significantly down-regulated in ccRCC, and loss of PDZK1 was correlated with higher TNM staging in TCGA database. Similar results were obtained by a tissue microarray study of ccRCC patient specimens. Importantly, loss of PDZK1 was remarkably correlated with poor prognosis of ccRCC patients.

As we know, VHL-HIF-1α pathway has a critical role in ccRCC. To investigate whether VHL-HIF-1α pathway is involved in PDZK1-mediated inhibition on the development and progression of ccRCC, cell lysates of 769-P and 786-O were immunoblotted, respectively, to detect HIF-1α expression, and no detectable expression of HIF-1α was observed in either 769-P and 786-O cells (Supplementary Figure S6a). GSEA results show that PDZK1 expression has no correlation with gene signatures of HIF-1/2α signaling activation in clinical ccRCC specimens (Supplementary Figure S6b and c), indicating that PDZK1 inhibits the development and progression of ccRCC probably independent of VHL-HIF pathway.

In conclusion, PDZK1 is identified as a novel tumor suppressor in ccRCC and has been demonstrated its inhibition on proliferation, migration and invasion by targeting SHP-1. Loss of PDZK1 expression is correlated with SHP-1 activation and poor clinical outcomes in ccRCC. Taken together, our findings provide novel clues for understanding of ccRCC carcinogenesis.

MATERIALS AND METHODS

Reagents and antibodies
NSC-87877 (565851), a SHP-1 selective inhibitor, was purchased from Calbiochem (Millipore, Billerica, MA, USA). The following antibodies were purchased: anti-His antibody from MBL (Nagoya, Japan), anti-Myc antibody from Applygen (Beijing, China), anti-PDZK1 antibody and anti-phosphor-SHP-1 (Tyr536) antibody from Abcam (Cambridge, UK), anti-PLCβ3 and anti-SHP-1 from Santa Cruz (Dallas, TX, USA), anti-FLAG M2 antibody and FLAG M2-agarose from Sigma (St Louis, MO, USA), anti-STAT5, anti-phosphor-STAT5 (Tyr694), anti-STAT3, anti-phosphor-STAT3 (Tyr705), anti-phosphor-Akt (Ser473) and anti-Akt from CST (Danvers, MA, USA), HRP-conjugated secondary antibodies and anti-GAPDH from ZSGB-BIO (Beijing, China).

Data sets collection and ccRCC patient samples
Totally six ccRCC tissues and matched adjacent renal tissues were collected from the First Hospital of Shanxi Medical University of Taiyuan during 2010. Patients who signed the informed consents were included. This study has been approved by Ethics Committee of Shanxi Medical University. The tissue microarrays of ccRCC, containing biopsies from 90 ccRCC and its adjacent renal tissues, were purchased from Shanghai Outdo Biotech (Shanghai, China).

The GEO data set GSE53757, which consisted of 72 paired renal cancer and adjacent renal tissues, was used for the differential expression genes screening and GO analyses. TCGA ccRCC RNA-Seq and matching clinical data were collected from Synapse website (http://synapse.org; syn1461159). RNA-Seq analysis was performed with the TCGA data of 531 ccRCC and 72 adjacent renal tissues.

GEO2R and GO analyses
GEO2R analyzer, a software tool for analyzing the data in GEO database, was used to analyze the public available GSE53757 data.[32] A total of 144 samples were divided into two groups: 72 ccRCC tissues and 72 matched adjacent renal tissues. The cutoff criteria for screening differentially-expressed mRNAs was: $P < 0.05$ and the fold change of expression levels > 2.0. To explore the functional annotation enrichment of genes, the GO analyses were performed with DAVID tools (http://david.abcc.ncifcrf.gov/).

Gene set enrichment analysis
GSEA was carried out as previously[33] to assess user-defined gene sets described as follows: SHP-1 activation gene set was defined as genes upregulated at least 1.5-fold changes associated with stimulation of SHP-1 PTPase activities (GSE42922). Akt signaling gene set (HALLMARK_PI3-K_Akt_SIGNALING) and STAT3 signaling gene set (AZARE_STAT3_TARGETS)

were obtained from Molecular Signatures Database from the Broad Institute (http://software.broadinstitute.org/gsea/msigdb). Tests were performed by using the default settings, and permutations number was set at 1000. False discovery rate < 0.25 was considered statistically significant.

Immunohistochemistry
The samples used for immunohistochemistry analysis include tissue microarray of human tissues, and mice tumor xenograft. Immunohistochemistry was performed as described previously.[34] Primary antibodies were incubated at the optimal conditions (PDZK1, 1:100, Abcam; pSHP-1, 1:100, Abcam; Ki67, 1:100, Santa Cruz). Omitting primary antibodies were used as negative control. IPP software was used to analyze optical densitometry.

Cell culture and transfection
COS7 and HEK293 cells were purchased from European Collection of Animal Cell Culture (ECACC, Porton Down, Salisbury, UK). The human renal carcinoma cell lines 769-P, 786-O and ACHN were obtained from American Type Culture Collection (ATCC, Manassas, VA, USA). Cells were grown in DMEM medium (COS7 and HEK293) or RPMI-1640 medium (769-P, 786-O and ACHN) containing 10% fetal bovine serum (complete medium) and 1% streptomycin/ penicillin, at 37 °C and 5% CO_2. All cell culture reagents were provided by HyClone (Logan, UT, USA). Cells were transfected by using Lipofecamine 2000 (Invitrogen, Carlsbad, CA, USA). For cell stable transfection, PDZK1 plasmid and control vector were transfected into 786-O, 769-P or ACHN cells and screened with G418 (800 mg/ml; Amresco, Solon, OH, USA). For stable knockdown transfection, shPDZK1 plasmid and shControl vector were transfected into 786-O or 769-P cells. Stably transfected cells were selected by using 300 ng/ml puromycin (Sigma).

Plasmid constructions and RNA interference
The constructs encoding Myc-PDZK1, Flag-PLCβ3, GST-PLCβ3-CT, GST-PDZK1-PDZ1 and His-PDZK1-PDZ1 were generously supplied by Dr Randy Hall (Emory University, GA, USA). The PLCβ3-CT is comprised of the C-Terminal 50 amino acids of human PLCβ3. The construct of C-terminal PDZ-binding motif (NTQL)-deleted PLCβ3 was derived from Flag-PLCβ3 by PCR and verified by bidirectional sequencing.

Small interfering RNA (siRNA) duplexes were synthesized by Sigma-Aldrich and the siRNA sequences were as below:

PDZK1 siRNA-#1, sense 5′-CAAAGAAACUGACAAGCGUdTdT-3′ and anti-sense 5′-ACGCUUGUCAGUUUCUUUGdTdT-3′; PDZK1 siRNA-#2, sense 5′-GUCAAAUCAUCAAGGACAUdTdT-3′ and anti-sense 5′-AUGUCCUUGAU GAUUUGACdTdT-3′; SHP-1 siRNA-#1, sense 5′-GCAUGACACAACCGAAUA Ctt-3′ and anti-sense 5′-GUAUUCGGUUGUGUCAUGCtc-3′; SHP-1 siRNA-#2, sense 5′-GGUGACCCAUAUUCGGAUCtt-3′ and anti-sense 5′-GAUCCGAAUA UGGGUCACCtg-3′. The control siRNA (sc-37007) and siRNA against PLCβ3 (sc-36272) were obtained from Santa Cruz Biotechnology. The plasmids of shPDZK1#1 and shPDZK1#2 which are employed to stable knockdown of PDZK1 were kindly offered by Dr Michael R Beard.[27]

Cell proliferation measurement
Cells were seeded in 96-well plates (3000 cells per well). Plates were then incubated for 24-72 h, and viable cells were analyzed with Cell Counting Kit-8 (Dojindo, Kumamoto, Japan) by using a Enspire, microplate reader (Perkin Elmer, Waltham, MA, USA) at 450 nm.

Colony formation assay
Cells were digested into a single cell suspension and seeded in six-well plates (300 cells per well). After incubation for 14 days, cells were stained with crystal violet, and then the colonies (> 50 cells) were counted.

Cell cycle analysis
Cell cycles were examined by flow cytometry. After fixing for 30 min in cold ethanol, cells were then incubated with propidium iodide for 30 min before flow cytometry (BD Biosciences, San Jose, CA, USA) analysis.

Cell migration and invasion assay
Cell migration was performed with in vitro scratch assay as previously described.[35] The invasion assay was determined using modified Boyden chambers coated with Matrigel in 24-well plate (Becton-Dickinson Biosciences, Bedford, MA, USA).

In vivo xenograft formation assay

The study was approved by the Capital Medical University Animal Care and Use Committee. ACHN cells stable transfected with PDZK1 or vector control were subcutaneously implanted into the dorsal flank in each of Balb/c nude mice (4–5 weeks) (1×10^5 cells in 0.1 ml PBS). Each group included 12 mice. The mice were monitored every two days for the growth of tumors, and they were killed after 5 weeks. The tumor xenografts were dissected and weighted after the deaths of the mice. Tumor volumes were estimated according to the equation: volume = width (mm) × width (mm) × length (mm)/2.

GST pull down, co-immunoprecipitation and western blotting

Purification of GST- or His-tagged proteins and GST pull down assay, lysis of cells and tumor samples, co-immunoprecipitation and immunoblotting were carried out as described previously.[36]

Statistical analysis

The statistics software of the SPSS (SPSS Inc, Chicago, IL, USA), or Graphpad Prism 5.0 (Graphpad Software, Inc., La Jolla, CA, USA) were used in this study. P-value < 0.05 was considered statistically significant.

CONFLICT OF INTEREST

The authors declare no conflict of interest.

REFERENCES

1 Ljungberg B, Campbell SC, Choi HY, Jacqmin D, Lee JE, Weikert S et al. The epidemiology of renal cell carcinoma. Eur Urol 2011; 60: 615–621.

2 Lopez-Beltran A, Scarpelli M, Montironi R, Kirkali Z. 2004 WHO classification of the renal tumors of the adults. Eur Urol 2006; 49: 798–805.

3 Ciccarese C, Brunelli M, Montironi R, Fiorentino M, Iacovelli R, Heng D et al. The prospect of precision therapy for renal cell carcinoma. Cancer Treat Rev 2016; 49: 37–44.

4 Moch H, Montironi R, Lopez-Beltran A, Cheng L, Mischo A. Oncotargets in different renal cancer subtypes. Curr Drug Targets 2015; 16: 125–135.

5 Klatte T, Seligson DB, Riggs SB, Leppert JT, Berkman MK, Kleid MD et al. Hypoxia-inducible factor 1 alpha in clear cell renal cell carcinoma. Clin Cancer Res 2007; 13: 7388–7393.

6 Rathmell WK, Chen S. VHL inactivation in renal cell carcinoma: implications for diagnosis, prognosis and treatment. Expert Rev Anticancer Ther 2008; 8: 63–73.

7 Calvo E, Schmidinger M, Heng DY, Grunwald V, Escudier B. Improvement in survival end points of patients with metastatic renal cell carcinoma through sequential targeted therapy. Cancer Treat Rev 2016; 50: 109–117.

8 Caceres W, Cruz-Chacon A. Renal cell carcinoma: molecularly targeted therapy. P R Health Sci J 2011; 30: 73–77.

9 Kroeze SG, Bijenhof AM, Bosch JL, Jans JJ. Diagnostic and prognostic tissuemarkers in clear cell and papillary renal cell carcinoma. Cancer Biomark 2010; 7: 261–268.

10 Subbaiah VK, Kranjec C, Thomas M, Banks L. PDZ domains: the building blocks regulating tumorigenesis. Biochem J 2011; 439: 195–205.

11 Kanamori M, Sandy P, Marzinotto S, Benetti R, Kai C, Hayashizaki Y et al. The PDZ protein tax-interacting protein-1 inhibits beta-catenin transcriptional activity and growth of colorectal cancer cells. J Biol Chem 2003; 278: 38758–38764.

12 Polette M, Gilles C, Nawrocki-Raby B, Lohi J, Hunziker W, Foidart JM et al. Membrane-type 1 matrix metalloproteinase expression is regulated by zonula occludens-1 in human breast cancer cells. Cancer Res 2005; 65: 7691–7698.

13 Yao S, Zheng P, Wu H, Song LM, Ying XF, Xing C et al. Erbin interacts with c-Cbl and promotes tumourigenesis and tumour growth in colorectal cancer by preventing c-Cbl-mediated ubiquitination and down-regulation of EGFR. J Pathol 2015; 236: 65–77.

14 Saponaro C, Malfettone A, Dell'Endice TS, Brunetti AE, Achimas-Cadariu P, Paradiso A et al. The prognostic value of the Na(+)/ H(+) exchanger regulatory factor 1 (NHERF1) protein in cancer. Cancer Biomark 2014; 14: 177–184.

15 Walsh DR, Nolin TD, Friedman PA. Drug Transporters and Na+/H+ Exchange Regulatory Factor PSD-95/Drosophila Discs Large/ZO-1 Proteins. Pharmacol Rev 2015; 67: 656–680.

16 Li H, Zhang B, Liu Y, Yin C. EBP50 inhibits the migration and invasion of human breast cancer cells via LIMK/cofilin and the PI3K/Akt/mTOR/MMP signaling pathway. Med Oncol 2014; 31: 162.

17 Gardiol D. PDZ-containing proteins as targets in human pathologies. FEBS J 2012; 279: 3529.

18 Cooper SJ, Zou H, Legrand SN, Marlow LA, von Roemeling CA, Radisky DC et al. Loss of type III transforming growth factor-beta receptor expression is due to methylation silencing of the transcription factor GATA3 in renal cell carcinoma. Oncogene 2010; 29: 2905–2915.

19 Zheng J, Wang L, Peng Z, Yang Y, Feng D, He J. Low level of PDZ domain containing 1 (PDZK1) predicts poor clinical outcome in patients with clear cell renal cell carcinoma. EBioMedicine 2017; 15: 62–72.

20 Rodriguez-Ubreva FJ, Cariaga-Martinez AE, Cortes MA, Romero-De Pablos M, Ropero S, Lopez-Ruiz P et al. Knockdown of protein tyrosine phosphatase SHP-1 inhibits G1/S progression in prostate cancer cells through the regulation of components of the cell-cycle machinery. Oncogene 2010; 29: 345–355.

21 Poole AW, Jones ML. A SHPing tale: perspectives on the regulation of SHP-1 and SHP-2 tyrosine phosphatases by the C-terminal tail. Cell Signal 2005; 17: 1323–1332.

22 Xiao W, Ando T, Wang HY, Kawakami Y, Kawakami T. Lyn- and PLC-beta3-dependent regulation of SHP-1 phosphorylation controls Stat5 activity and myelomonocytic leukemia-like disease. Blood 2010; 116: 6003–6013.

23 Sharma Y, Ahmad A, Bashir S, Elahi A, Khan F. Implication of protein tyrosine phosphatase SHP-1 in cancer-related signaling pathways. Future Oncol 2016; 12: 1287–1298.

24 Kim JK, Kwon O, Kim J, Kim EK, Park HK, Lee JE et al. PDZ domain-containing 1 (PDZK1) protein regulates phospholipase C-beta3 (PLC-beta3)-specific activation of somatostatin by forming a ternary complex with PLC-beta3 and somatostatin receptors. J Biol Chem 2012; 287: 21012–21024.

25 Ghosh MG, Thompson DA, Weigel RJ. PDZK1 and GREB1 are estrogen-regulated genes expressed in hormone-responsive breast cancer. Cancer Res 2000; 60: 6367–6375.

26 Inoue J, Otsuki T, Hirasawa A, Imoto I, Matsuo Y, Shimizu S et al. Overexpression of PDZK1 within the 1q12-q22 amplicon is likely to be associated with drug-resistance phenotype in multiple myeloma. Am J Pathol 2004; 165: 71–81.

27 Eyre NS, Drummer HE, Beard MR. The SR-BI partner PDZK1 facilitates hepatitis C virus entry. PLoS Pathog 2010; 6: e1001130.

28 Stebbing J, Lit LC, Zhang H, Darrington RS, Melaiu O, Rudraraju B et al. The regulatory roles of phosphatases in cancer. Oncogene 2014; 33: 939–953.

29 Montano X. Repression of SHP-1 expression by p53 leads to trkA tyrosine phosphorylation and suppression of breast cancer cell proliferation. Oncogene 2009; 28: 3787–3800.

30 Sooman L, Ekman S, Tsakonas G, Jaiswal A, Navani S, Edqvist PH et al. PTPN6 expression is epigenetically regulated and influences survival and response to chemotherapy in high-grade gliomas. Tumour Biol 2014; 35: 4479–4488.

31 Golebiewska U, Scarlata S. The effect of membrane domains on the G protein-phospholipase Cbeta signaling pathway. Crit Rev Biochem Mol Biol 2010; 45: 97–105.

32 Barrett T, Wilhite SE, Ledoux P, Evangelista C, Kim IF, Tomashevsky M et al. NCBI GEO: archive for functional genomics data sets--update. Nucleic Acids Res 2013; 41: D991–D995.

33 Subramanian A, Tamayo P, Mootha VK, Mukherjee S, Ebert BL, Gillette MA et al. Gene set enrichment analysis: a knowledge-based approach for interpreting genome-wide expression profiles. Proc Natl Acad Sci USA 2005; 102: 15545–15550.

34 Du Y, Liu L, Wang C, Kuang B, Yan S, Zhou A et al. TACC3 promotes colorectal cancer tumourigenesis and correlates with poor prognosis. Oncotarget 2016; 7: 41885–41897.

35 Ma Q, Yang Y, Feng D, Zheng S, Meng R, Fa P et al. MAGI3 negatively regulates Wnt/beta-catenin signaling and suppresses malignant phenotypes of glioma cells. Oncotarget 2015; 6: 35851–35865.

36 Sun L, Zheng J, Wang Q, Song R, Liu H, Meng R et al. NHERF1 regulates actin cytoskeleton organization through modulation of alpha-actinin-4 stability. FASEB J 2016; 30: 578–589.

Supplementary Information accompanies this paper on the Oncogene website (http://www.nature.com/onc)